THE JOURNAL OF BIOLOGICAL CHEMISTRY VOL. 290, NO. 9, pp. 5470–5483, February 27, 2015

Transfected Poly(I:C) Activates Different dsRNA Receptors, Leading to Apoptosis or Immunoadjuvant Response in Androgen-independent Prostate Cancer Cells*

Received for publication, July 31, 2014, and in revised form, November 29, 2014 Published, JBC Papers in Press, January 8, 2015, DOI 10.1074/jbc.M114.601625

Sara Palchetti[‡], Donatella Starace[‡1], Paola De Cesaris[§], Antonio Filippini[‡], Elio Ziparo[‡], and Anna Riccioli[‡2]

From the [‡]Istituto Pasteur-Fondazione Cenci Bolognetti, Department of Anatomy, Histology, Forensic Medicine, and Orthopedics, Section of Histology and Medical Embryology, "Sapienza" University of Rome, Rome, Italy and the [§]Department of Biotechnological and Applied Clinical Sciences, University of L'Aquila, L'Aquila, Italy

Background: Castration-resistant prostate cancer (CRPC) is refractory to chemo-radiotherapy.
Results: Transfection of the synthetic analog of dsRNA poly(I:C) simultaneously stimulates apoptosis and IFN-β expression through different pathways in androgen-independent prostate cancer (PCa) cells.
Conclusion: Dual parallel pathways triggered by distinct receptors activate direct and immunologically mediated antitumor effects in advanced PCa.
Significance: The proapoptotic/immunoadjuvant poly(I:C)-Lipofectamine complex may offer new therapeutic insights into CRPC.

Despite the effectiveness of surgery or radiation therapy for the treatment of early-stage prostate cancer (PCa), there is currently no effective strategy for late-stage disease. New therapeutic targets are emerging; in particular, dsRNA receptors Toll-like receptor 3 (TLR3) and cytosolic helicases expressed by cancer cells, once activated, exert a pro-apoptotic effect in different tumors. We previously demonstrated that the synthetic analog of dsRNA poly(I:C) induces apoptosis in the androgen-dependent PCa cell line LNCaP in a TLR3-dependent fashion, whereas only a weak apoptotic effect is observed in the more aggressive and androgen-independent PCa cells PC3 and DU145. In this paper, we characterize the receptors and the signaling pathways involved in the remarkable apoptosis induced by poly(I:C) transfected by Lipofectamine (in-poly(I:C)) compared with the 12-fold higher free poly(I:C) concentration in PC3 and DU145 cells. By using genetic inhibition of different poly(I:C) receptors, we demonstrate the crucial role of TLR3 and Src in in-poly(I:C)-induced apoptosis. Therefore, we show that the increased in-poly(I:C) apoptotic efficacy is due to a higher binding of endosomal TLR3. On the other hand, we show that in-poly(I:C) binding to cytosolic receptors MDA5 and RIG-I triggers IRF3-mediated signaling, leading uniquely to the up-regulation of IFN-β, which likely in turn induces increased TLR3, MDA5, and RIG-I proteins. In summary, in-poly(I:C) activates two distinct antitumor pathways in PC3 and DU145 cells: one mediated by the TLR3/Src/STAT1 axis, leading to apoptosis, and the other one mediated by MDA5/RIG-I/IRF3, leading to immunoadjuvant IFN-β expression.

Prostate cancer (PCa)[3] represents the second leading cause of cancer death in men and develops as a result of the accumulation of genetic and epigenetic alterations. PCa is initially treated with removal of androgens; however, androgen depletion is usually associated with the recurrence of metastatic and more aggressive PCa termed "castration-resistant" or androgen- and chemotherapy-insensitive (1). Data from the literature suggest that new therapeutic targets are emerging, and among these targets, an important role is played by the Toll-like receptor (TLR) family (2). This family includes several membrane-bound receptors that recognize pathogen-associated molecular patterns and represents the first line of defense against invading pathogens. TLRs transduce the signal through MAPKs, NF-κB, and IRF3 (interferon regulatory factor-3), which induce the transcription of proinflammatory cytokines and type I interferons (3). TLRs are expressed both by immune cells and by cancer cells; thus, the use of specific TLR agonists alone or in combination with standard chemo- or radiotherapies has been shown to have a valid anti-cancer activity in different *in vitro* or *in vivo* cancer models, and several molecules have been tested in clinical trials (4). In particular, it is known that the activation of Toll-like receptor 3 (TLR3) by the dsRNA synthetic analog poly(I:C) has a proapoptotic and thus antitumoral effect in different tumors (5). It is well known that extracellular dsRNA, produced as viral genome or genomic intermediate by dead infected cells, is endocytosed and recognized by TLR3 (6), which is located on the endosomal membrane. TLR3 uses the adaptor protein TRIF (7), engaging the protein kinase IKK, to activate the transcription factor NF-κB and the protein kinases TBK1/IKK-ϵ (8) to activate the transcription factors IRF3 and IRF7 (9). Moreover, it has been demonstrated that the

* This work was supported by the Italian Ministry of University and Research (MIUR) Grant prot.2010MCLPLB, a grant from Fondazione Roma (to E. Z.), and Ricerca Scientifica Ateneo "Sapienza" 2014 (to E. Z.).

[1] To whom correspondence may be addressed: DAHFMO-Unit of Histology and Medical Embryology, Sapienza University of Rome, Via Antonio Scarpa 16, 00161 Rome, Italy. Tel.: 39-06-4976-6582; Fax: 39-06-446-2854; E-mail: donatella.starace@uniroma1.it.

[2] To whom correspondence may be addressed: DAHFMO-Unit of Histology and Medical Embryology, Sapienza University of Rome, Via Antonio Scarpa 16, 00161 Rome, Italy. Tel.: 39-06-4976-6239; Fax: 39-06-446-2854; E-mail: anna.riccioli@uniroma1.it.

[3] The abbreviations used are: PCa, prostate cancer; poly(I:C), polyinosinic-polycytidylic acid; in-poly(I:C), poly(I:C) transfected by Lipofectamine; ex-poly(I:C), free poly(I:C); RLH, RIG-I-like helicase; PKR, double-stranded RNA-dependent protein kinase; TLR, Toll-like receptor; MTT, 3-(4,5-dimethylthiazol-2-yl)-2,5-diphenyltetrazolium bromide; PI, propidium iodide; IFNR, type I interferon receptor; Pepinh-TRIF, TRIF inhibitor peptide.

tyrosine kinase Src is activated by dsRNA, associates with TLR3, and is essential for dsRNA-elicited IRF3 and STAT1 activation (10). In contrast, intracellular dsRNA produced by viruses replicating in the cytoplasm is recognized by cytosolic sensors, including double-stranded RNA-dependent protein kinase (PKR) as well as RIG-I (retinoic inducible gene-I) and MDA5 (melanoma differentiation-associated gene 5), which are collectively called RIG-I-like helicases (RLHs) (11, 12). The RLHs use mitochondrial membrane-bound protein, MAVS (mitochondrial antiviral signaling protein; also known as IPS-1, VISA, or Cardif), as an adaptor that recruits several members of the TRAF family proteins, which, in turn, activate the same protein kinases and transcription factors as TLR3 (13–16). These transcription factors drive the expression of type I interferon genes and many interferon-stimulated genes, which are essential for both direct virus elimination and immunologically mediated antiviral defense (17). We previously demonstrated that poly(I:C) (specific ligand of TLR3) induces apoptosis in the androgen-dependent prostate cancer cell line LNCaP in a TLR3-dependent fashion, whereas it has been observed to have a weaker apoptotic effect in the more aggressive and androgen-independent prostate cancer cell lines PC3 (18) and DU145 (19). Recently, Matsushima-Miyagi *et al.* (20) demonstrated that non-replicating Sendai intracellular virus particles induce cancer-selective apoptosis via the up-regulation of TRAIL and Noxa downstream of the RIG-I/MAVS pathway in prostate cancer cell lines. In this regard, we have recently demonstrated that the encapsulation of poly(I:C) with three different formulations of cationic liposomes was up to 10 times more efficient than the free drug in eliminating both PC3 and DU145 metastatic prostate cancer cells (21). In the present work, we analyzed the mechanisms involved in the induction of apoptosis induced by poly(I:C) transfected by Lipofectamine (the most commonly used transfection agent) compared with free poly(I:C) in PC3 and DU145 cells. Here we demonstrate that, when poly(I:C) is complexed with Lipofectamine, its delivery into the cell is not directly to the cytosol, but, once internalized, poly(I:C) first makes contact with endosomes, where TLR3 is localized, and only subsequently is it released in the cytosol where it interacts with cytosolic receptors. Consequently, we aimed to dissect the signaling pathways triggered by both TLR3 and cytosolic receptors and their downstream biological responses in two aggressive androgen-resistant PCa cell lines. Altogether, our results highlighted dual distinct antitumor pathways activated by transfected poly(I:C): one mediated by TLR3, Src-dependent and leading to apoptosis, and the other one mediated by the cytosolic receptors MDA5 and RIG-I, IRF3-dependent, leading to up-regulation of MDA5, RIG-I, TLR3, and IFN-β production. Finally, we show that the higher levels of apoptosis induced by in-poly(I:C) compared with ex-poly(I:C) are dependent on different magnitude of TLR3 stimulation due to a greater delivery in the endosomes rather than to the trigger of distinct apoptotic pathways.

EXPERIMENTAL PROCEDURES

Cell Lines and Reagents—PC3 and DU145 cell lines, derived from human bone and brain prostate cancer metastasis, respectively, were purchased from ATCC (Manassas, VA). PC3 cells were maintained in RPMI medium, and DU145 cells were maintained in minimum essential medium Eagle. Both media were supplemented with 2 mM L-glutamine, 100 IU/ml penicillin-streptomycin, 1 mM sodium pyruvate, 10 mM Hepes, 1.5 mg/liter sodium bicarbonate, and 10% fetal bovine serum (FBS) (Sigma-Aldrich).

Poly(I:C), poly(I:C)-rhodamine, TRIF inhibitor peptide (Pep-inh-TRIF), 2-aminopurine, and BX795 were from Invivogen (San Diego, CA). SU6656, SB203580, SP600125, and benzyloxycarbonyl-VAD-fluoromethyl ketone were from Calbiochem (Merck KGaA). Propidium iodide and 3-(4,5-dimethylthiazol-2-yl)-2,5-diphenyltetrazolium bromide (MTT) were from Sigma-Aldrich. IKK-ϵ kinase inhibitor II was from Biovision (Milpitas, CA). Early and late endosomes-GFP were from Invitrogen.

Caspase Activity Assay—PC3 and DU145 cells were treated with poly(I:C) alone or in combination with Lipofectamine, and after 48 and 72 h, cells were detached with trypsin/EDTA and centrifuged at 1000 rpm for 5 min at 4 °C. The pellet was resuspended in 50 μl of cell lysis buffer provided by caspase-8 and -9 activity kits (Biovision). After determination of protein concentration, 150 μg of protein were incubated in 96-plate well with reaction buffer and IETD-*p*-nitroanilide substrate (caspase-8) or LEHD-*p*-nitroanilide substrate (caspase-9). After 2 h of incubation at 37 °C the samples were read at 405 nm. The -fold increase in caspase activity was determined by comparing the levels of treated samples with the level of the control.

Apoptosis Assays—For propidium iodide (PI) staining, cells were detached with trypsin/EDTA, washed twice with cold phosphate-buffered saline (PBS), and then fixed in 70% ethanol for 24 h. After washing three times with PBS, cells were incubated with 50 μg/ml PI for 3 h at room temperature before FACS analysis by a Coulter Epics XL flow cytometer (Beckman Coulter, Fullerton, CA). Cells were gated using forward *versus* side scatter to exclude debris. The percentage of cells in the sub-G_1 compartment was considered apoptotic (using WinMDI software).

Mitochondrial Membrane Potential Measurement—Dissipation of the mitochondrial membrane potential is a hallmark for intrinsic apoptosis. Mitochondrial membrane potential was analyzed using JC-1 dye staining (Immunological Sciences). The cationic dye JC-1 stains the mitochondria of healthy cells red and apoptotic cells green. JC-1 (5 mg/ml) stock solution was diluted in RPMI, and 1×10^6 cells were diluted in JC-1/RPMI medium and incubated for 15 min in the dark at 37 °C. Cells were washed twice in 1× PBS and then analyzed for red and green fluorescence by flow cytometry.

Analysis of Cell Viability—For the MTT assay, 2×10^4 PC3 and DU145 cells were seeded on 96-well plates. After 24 h, cells were treated with poly(I:C) and Lipofectamine at increasing doses for 24 and 48 h. Cell viability was assessed by MTT (Sigma-Aldrich), as described (22). Briefly, PC3 and DU145 cells were seeded on 96-well plates and after 24 h were treated with poly(I:C) complexed with Lipofectamine for 24 and 48 h. MTT was added to each well at the a concentration of 0.5 mg/ml, and after 4 h of incubation at 37 °C, the formazan salt was dissolved with 100 μl of isopropyl alcohol. The absorbance of each well was measured with an ELISA reader at 550-nm

wavelength, and the viability was calculated for each treatment as "OD of treated cells/OD of control cells" × 100.

Western Blotting—Cell lysates were prepared in cell lysis buffer (Cell Signaling, Danvers, MA). Protein concentration was determined by the microbicinchoninic acid method (Pierce).

Equal amounts of proteins (40 μg) were subjected to SDS-PAGE and transferred onto nitrocellulose membrane saturated with 5% nonfat dry milk in Tris-buffered saline with 0.1% Tween 20. Membranes were incubated with primary antibody and subsequently with horseradish peroxidase-conjugated secondary antibody for 1 h at room temperature. Membranes were washed with Tris-buffered saline with 0.1% Tween 20 and developed using the chemiluminescence system (ECL Advance, Amersham Biosciences). The sources of primary antibodies were as follows: cleaved caspase-3, TLR3, MDA5, RIG-I, MAVS, phospho-IRF3, phospho-JNK, and phospho-p38 from Cell Signaling (Danvers, MA); IRF3 from Santa Cruz Biotechnology, Inc.; phospho-PKR and phospho-STAT1 Tyr^{701} from Abcam (Cambridge, UK). β-Actin was from Sigma-Aldrich. Secondary antibodies were horseradish peroxidase-conjugated goat anti-mouse or anti-rabbit (Bio-Rad).

Transfection—Poly(I:C) was transfected at a concentration of 2 μg/ml using 4 μg/ml Lipofectamine (Invitrogen) according to the manufacturer's protocol. siRNAs were transfected with Oligofectamine or Lipofectamine 2000 (Invitrogen) for 4 h: siMAVS targeted sequence, 5′-GAAUGCCUCUCCUGUUGCA-3′; siIRF3 targeted sequence, 5′-UUGACCAUCACGAGCCUCUUGGUCCAC-3′; siMDA5 targeted sequence, 5′-GUGGAAUACCCAUUCGACAUCUUUCUU-3′; siRIG-I targeted sequence, 5′-UAAGGUUGUUCACAAGAAUCUGUGG. TLR3 knockdown in PC3 and DU-145 cells was achieved by using TLR3-dominant negative plasmid (DN-TLR3, pZERO bearing the human TLR3ΔTIR gene; InvivoGen).

Stably transfected DN-TLR3 PC3 and control P-PURO PC3 cells were obtained as described previously (23). DU145 cells were transiently transfected with DN-TLR3 and control P-PURO for 48 h, and then cells were treated with poly(I:C) alone or in combination with Lipofectamine. Total DNA was extracted using phenol/chloroform/isoamyl alcohol (25:24:1). To confirm the presence of DN-TLR3 plasmid, semiquantitative polymerase chain reaction (PCR) was performed using 1 μg of total DNA, specific primers (10 μM) (forward, 5′-GAACGTTCTTTTTCGCAACG-3′; reverse, 5′-CTCATTGTGCTGGAGGTTCA-3′), and 1.5 units of *Taq* DNA polymerase (Invitrogen). Data were normalized for the expression of β-actin.

Luciferase Assay—The IFNβ-pGL3 luciferase reporter was kindly provided by Professor John Hiscott (Vaccine and Gene Therapy Institute of Florida, Port St. Lucie, FL) (24).

One day after plating (2.5×10^5 cells/ml), cells were transfected by means of Lipofectamine Plus reagent (Invitrogen) with IFNβ-pGL3. Transfection was stopped after 5 h by changing medium with 10% FBS. After 18 h, cells were stimulated with 2 μg/ml poly(I:C) complexed with 4 μg/ml Lipofectamine for 3 h, followed by lysis using specific buffer (Promega, Madison, WI). Luciferase activity was assayed with a Berthold luminometer using a luciferase assay kit (Promega), according to the manufacturer's instructions. Data were normalized to protein concentration.

Laser-scanning Confocal Microscopy—PC3 cells were treated with rhodamine-labeled poly(I:C) at 2 μg/ml plus Lipofectamine or rhodamine-labeled ex-poly(I:C) (25 or 2 μg/ml) at the indicated times in the presence of GFP-labeled early endosome marker Rab5a or GFP-labeled late endosome marker Rab7a. Then cells were fixed in 4% paraformaldehyde in PBS for 20 min. Laser-scanning confocal microscopy experiments were performed with a Leica TCS SP2 (Leica Microsystems Heidelberg GmbH). Analysis of the co-localization between endosomes and poly(I:C) was performed using Manders' colocalization coefficient (25).

Statistical Analysis—Statistical differences were determined either by Student's *t* test for paired samples or by one-way analysis of variance followed by Student's *t* test with Bonferroni's correction. $p < 0.05$ was considered significant. Densitometric analysis was performed using ImageJ software (National Institutes of Health).

RESULTS

Caspase-dependent Apoptosis of Androgen-resistant PCa Cells Is Strongly Enhanced by Transfected Poly(I:C) Compared with Extracellular Poly(I:C)—A common strategy to lower the required dosage of antitumor drugs and improve their effectiveness is encapsulation (26).

Strong cytotoxic effects induced by poly(I:C)-cationic liposome complexes on various malignant epithelial cells were observed previously (27, 28). Because the PC3 and DU145 cell lines are two models of androgen-insensitive very aggressive metastatic PCa and they are weakly sensitive to high doses of free poly(I:C) (ex-poly(I:C)) (18, 19), PC3 and DU145 cells were stimulated with in-poly(I:C) and subjected to cell viability analysis by an MTT assay. We observed a strong reduction of cell viability in both cell lines (data not shown). To investigate whether poly(I:C) transfection is able to induce apoptosis, PC3 and DU145 cells were treated for 48 h with increasing doses of in-poly(I:C) and then stained with PI and subjected to cell cycle analysis by flow cytometry. The histograms in Fig. 1*A* show a dose-dependent increase of apoptosis in both cell lines with the highest efficiency at 2 μg/ml poly(I:C) in combination with a double dose of Lipofectamine, compared with the untransfected poly(I:C) at the same concentration and even compared with a 12-fold higher poly(I:C) concentration (25 μg/ml). A Western blot for cleaved caspase-3 further confirmed the higher rate of apoptosis after in-poly(I:C) compared with ex-poly(I:C) in both cell lines (Fig. 1, *B* and *C*). The two main branches of apoptosis, the intrinsic and the extrinsic pathways, are triggered, respectively, by the activation of caspase-9 and caspase-8 (29). Therefore, to clarify the nature of apoptosis caused by poly(I:C), we investigated caspase-8 and -9 activity with colorimetric assays. As shown in Fig. 1*D*, in-poly(I:C) is able to induce a significant activation of caspase-8 (48 h) and -9 (72 h) in both cell lines, whereas ex-poly(I:C) treatment activates only caspase-8. The caspase involvement in in-poly(I:C)-induced apoptosis was confirmed by using the broad spectrum caspase inhibitor benzyloxycarbonyl-VAD-fluoromethyl ketone (*z-VAD*) (Fig. 1*E*). Because changes in mitochondrial

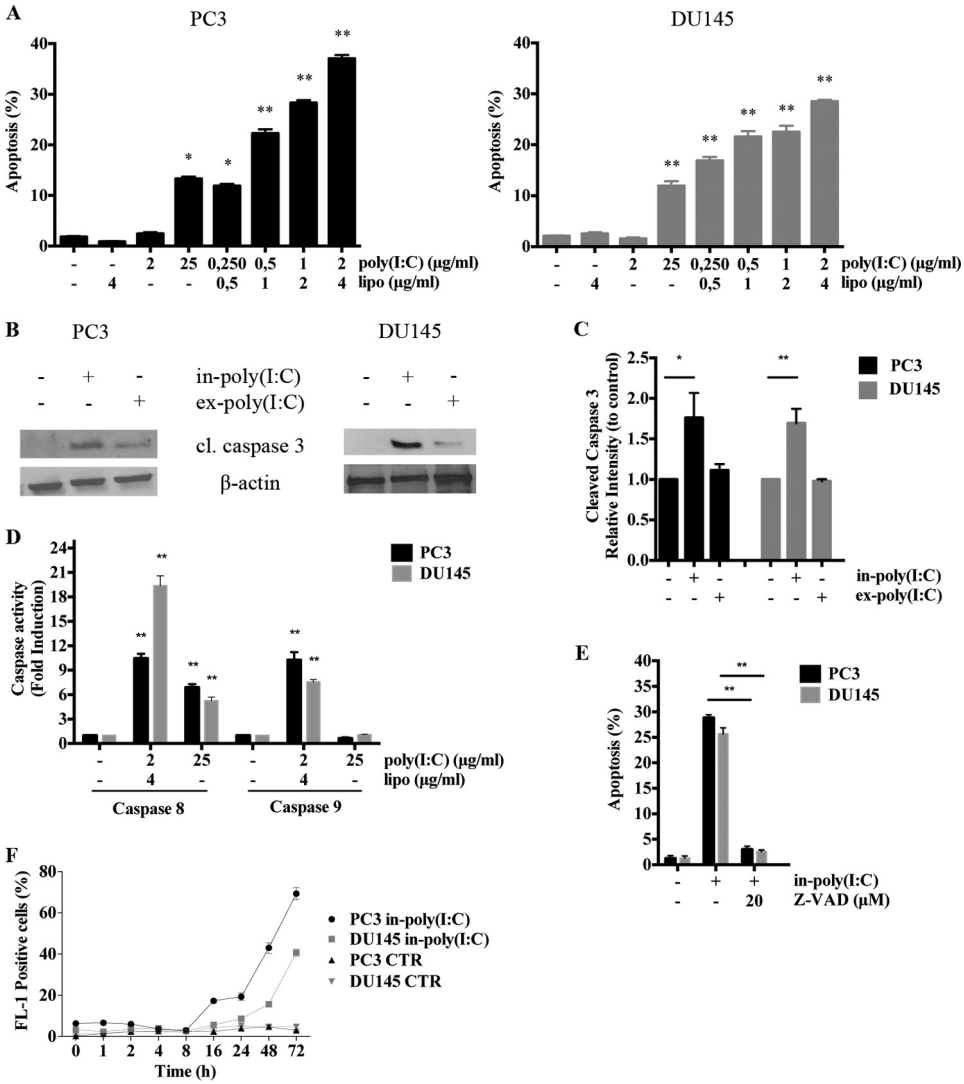

FIGURE 1. **Effects of poly(I:C) transfection on PC3 and DU145 cell death.** *A*, sub-G_1 analysis after PI staining of PC3 and DU145 cells stimulated for 48 h as indicated. Details of PI staining assay are described under "Experimental Procedures." Results represent means from three independent experiments with S.D. (*error bars*). The exact *p* values are reported *versus* respective controls (Student's paired *t* test): *, $p < 0.05$; **, $p < 0.01$. *B*, Western blot analysis for cleaved (*cl.*) caspase-3 of whole cell lysates obtained from PC3 and DU145 cells treated with poly(I:C) at 25 μg/ml added in medium (ex-poly(I:C)) or poly(I:C) at 2 μg/ml plus 4 μg/ml Lipofectamine (in-poly(I:C)) for 48 h. Data were normalized against β-actin. Data shown are from a typical experiment repeated three times with similar results. *C*, the histograms represent the densitometric values (mean ± S.D.) of protein levels from three different blots for cleaved caspase-3, calculated as the -fold increase in induction by comparing the values of poly(I:C)-treated with those of untreated cells (set arbitrarily at 1). Values were normalized against β-actin density values (Student's paired *t* test): *, $p < 0.05$; **, $p < 0.01$. *D*, PC3 and DU145 cells were treated with ex-poly(I:C) or in-poly(I:C) and then subjected to caspase-8 or -9 activity assays following the manufacturer's protocol. *E*, PC3 and DU145 were treated with in-poly(I:C) alone or in combination with pan-caspase inhibitor benzyloxycarbonyl-VAD-fluoromethyl ketone (*z-VAD*) at 20 μM for 48 h, and then cells were subjected to cell cycle analysis. The histograms represent the mean ± S.D. of three independent experiments (Student's paired *t* test; **, $p < 0.01$). *F*, JC1 assay on PC3 and DU145 cells. *FL-1*, flow cytometer channel for mitochondrial depolarization (percentage of positive cells). Details of the assays are described under "Experimental Procedures." Results represent the mean from three experiments with S.D. (*error bars*). The exact *p* values are reported *versus* the respective controls (Student's paired *t* test): *, $p < 0.05$; **, $p < 0.01$.

outer membrane permeability are critical to the progression of the intrinsic apoptotic pathway, we determined whether in-poly(I:C) treatment was able to induce mitochondria depolarization by using a JC-1 assay. We treated PC3 and DU145 cells with in-poly(I:C) at the indicated times; subsequently, cells were subjected to flow cytometry analysis to evaluate the percentage of depolarized-positive cells. Fig. 1*F* shows that in PC3 cells, poly(I:C) transfection induces mitochondrial depolarization starting from 16 h up to the maximum effect at 72 h, whereas in DU145 cells, the effect is delayed, starting from 48 h after in-poly(I:C) treatment, with the maximum effect after 72 h.

TLR3 Plays an Essential Role in Poly(I:C)-induced Apoptosis—To investigate which receptor is implicated in in-poly(I:C)-induced apoptosis, we first evaluated the implication of PKR, which has been demonstrated to be an active player in apoptosis induced by transfected dsRNA (30). Specific PKR inhibitor 2-aminopurine in combination with in-poly(I:C) does not affect apoptosis (data not shown). Because the RNA helicases MDA5 and RIG-I function as cytoplasmic sensors of viral RNA (12), we investigated MDA5 and RIG-I involvement in in-poly(I:C)-induced apoptosis. We first evaluated this by Western blot MDA5 and RIG-I protein levels, and, as shown in Fig. 2*A*, in-poly(I:C) induces up-regulation of these receptors in

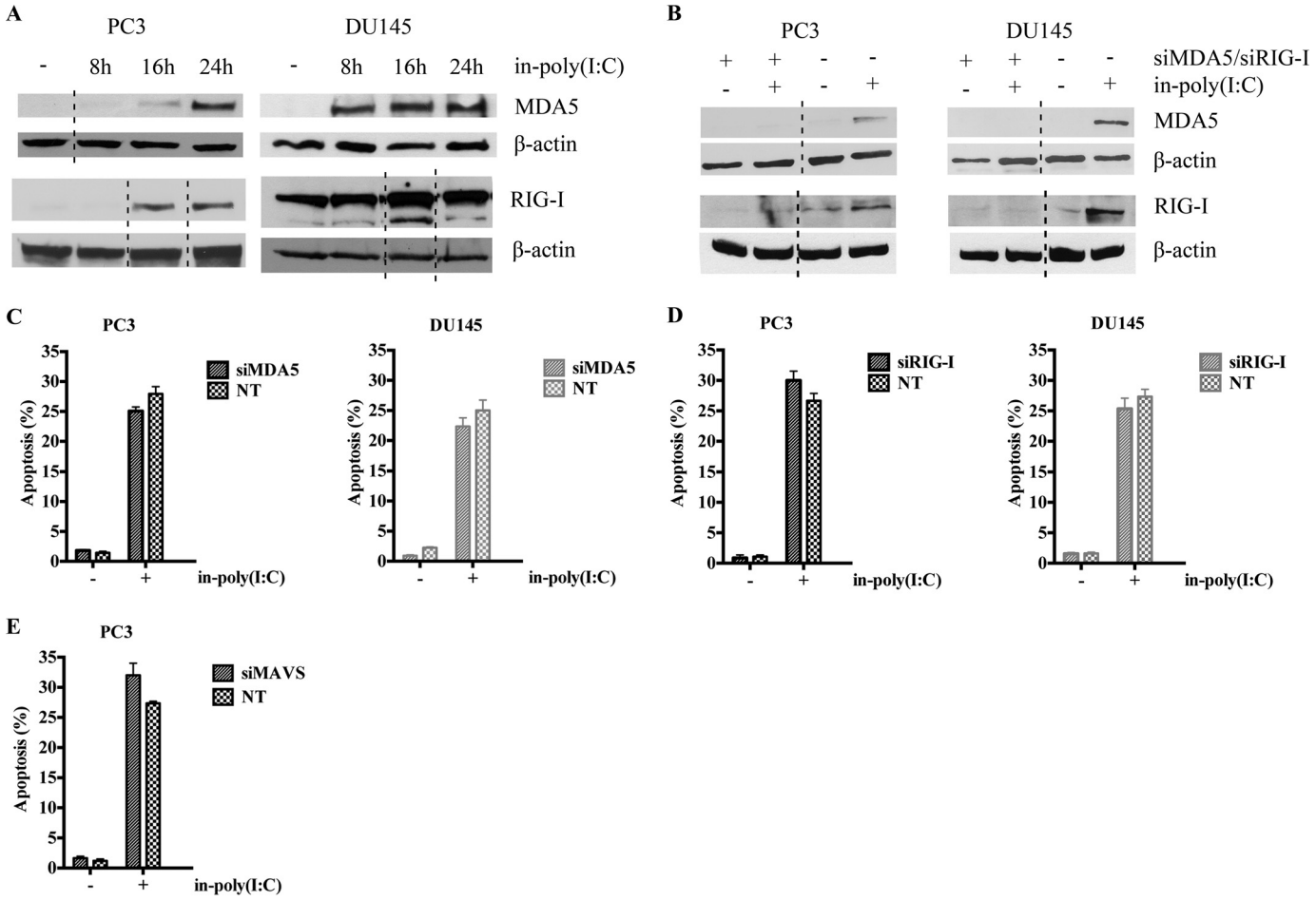

FIGURE 2. **MDA5, RIG-I, and MAVS are not implicated in apoptosis induced by transfected poly(I:C).** *A*, time course analysis of MDA5 and RIG-I assessed by Western blot of whole cell lysates obtained from PC3 and DU145 cells treated with in-poly(I:C). Data were normalized against *β*-actin. *B*, silencing of MDA5 or RIG-I was evaluated by Western blot analysis. PC3 and DU145 cells were treated with siRNA specific for MDA5 or RIG-I (*siMDA5* or *siRIG-I*) or with control siRNA (−) for 48 h. Subsequently, cells were treated with in-poly(I:C) for 48 h. Data were normalized against *β*-actin. *C* and *D*, PC3 and DU145 cells were treated with siMDA5 (*C*) or siRIG-I (*D*) or with control siRNA (*NT*) and subsequently with in-poly(I:C) for 48 h and then subjected to cell cycle analysis after PI incorporation. The histograms represent the mean ± S.D. (*error bars*) of the percentage of apoptotic cells of three independent experiments. The differences between NT and siMDA5 or siRIG-I are not significant. *E*, the histograms represent the apoptotic rate of PC3 treated with siMAVS or NT in combination of in-poly(I:C) after PI incorporation. The differences between NT and siMAVS are not significant. The histograms represent the mean ± S.D. of the percentage of apoptotic cells of three independent experiments. Data in *A* and *B* are representative of three Western blots from three independent experiments.

both cell lines, even though the underlying kinetics differ. To determine RNA helicase implication in in-poly(I:C)-induced apoptosis, we employed the siRNA approach. We confirmed by Western blot the silencing of MDA5 and RIG-I after using specific siRNAs in both cell lines (Fig. 2*B*). In in-poly(I:C)-treated cells, MDA5 and RIG-I knockdown *versus* control siRNA cells were shown not to significantly reduce apoptosis in the two cell lines, as assayed by PI incorporation (Fig. 2, *C* and *D*).

Because both helicases share the common downstream adapter MAVS (31), we silenced MAVS with specific siRNA in combination with in-poly(I:C) treatment in PC3 cells, and cell cycle analysis demonstrated that MAVS inhibition does not affect the apoptotic rate induced by in-poly(I:C) treatment (Fig. 2*E*).

Afterward, we hypothesized a possible role of TLR3 in poly(I:C)-induced apoptosis because data from the literature suggest that when poly(I:C) is internalized into cationic liposomes, once it enters into the cell, it may make contact with endosomes and then be carried to the cytoplasm (32, 33). We initially evaluated the TLR3 protein expression. Fig. 3*A* shows that in both PCa cell lines, TLR3 is up-regulated upon in-poly(I:C) stimulation in a time-dependent manner. We have previously reported in PC3 cells a low rate of TLR3-dependent apoptosis induced by ex-poly(I:C) (23). In order to determine whether TLR3 plays a role also in in-poly(I:C)-induced apoptosis, PC3 cells stably transfected with TLR3-dominant negative plasmid (DN-TLR3) and control plasmid (P-PURO) were treated with ex-poly(I:C) (as a control) or in-poly(I:C) and then subjected to cell cycle analysis. As shown in Fig. 3*B*, the apoptotic rate was completely reverted in DN-TLR3 PC3 cells after extracellular poly(I:C) treatment as expected, but, surprisingly, it was also strongly reduced after in-poly(I:C) treatment. Similarly, a marked apoptosis inhibition was obtained when DU145 cells were transiently transfected with DN-TLR3 plasmid (Fig. 3*C*) or were treated with Pepinh-TRIF to block TLR3 signal transduction (data not shown), suggesting a crucial role for TLR3 in in-poly(I:C)-dependent apoptosis in both PCa cell lines. PCR analysis with specific primers in Fig. 3, *D* and *E*, shows the presence of the pZERO-TLR3ΔTIR plasmid in DN-TLR3-

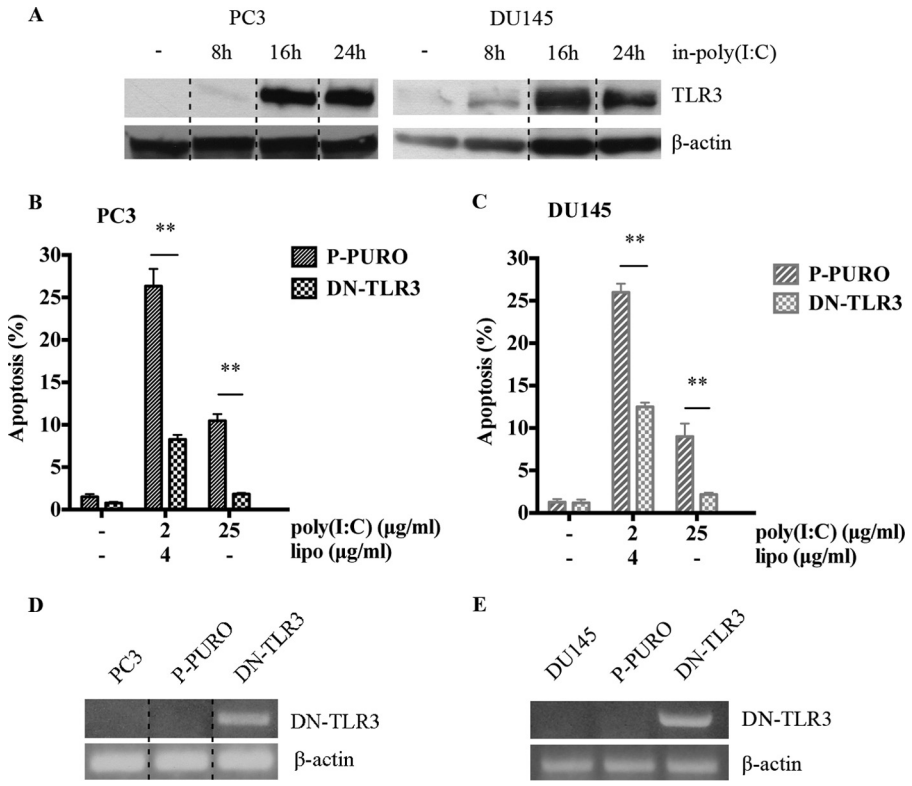

FIGURE 3. **TLR3 is crucial in poly(I:C)-induced apoptosis.** *A*, time course analysis by Western blot for TLR3 on whole cell lysates obtained from PC3 and DU145 cells treated with in-poly(I:C). Data are representative of three Western blots from three independent experiments. Data were normalized against *β*-actin. *B*, PC3 cells stably transfected with TLR3 dominant negative (DN-TLR3) and control plasmid (P-PURO) were treated with in-poly(I:C) or ex-poly(I:C) for 48 h and then subjected to cell cycle analysis after PI incorporation. *C*, DU145 cells were transiently transfected with DN-TLR3 or P-PURO, stimulated with in-poly(I:C) or ex-poly(I:C) for 48 h, and then subjected to cell cycle analysis. Results in *B* and *C* represent the mean from three independent experiments with S.D. (*error bars*). The exact *p* values are reported *versus* respective controls (Student's paired *t* test): **, $p < 0.01$. *D* and *E*, PC3 and DU145 cells transfected with DN-TLR3 or P-PURO were subjected to total DNA extraction, and the presence of the DN-TLR3 plasmid was assessed using PCR with specific primers (described under "Experimental Procedures"). Nontransfected cells were used as negative control. *β*-Actin was used as a control for equal amounts of DNA loaded.

PC3 and in DN-TLR3-DU145 cells (see "Experimental Procedures").

Transfection Strongly Increases Poly(I:C) Uptake and Endosomal Localization in Androgen-resistant PCa Cells—To demonstrate that the stronger apoptosis induced by in-poly(I:C) compared with ex-poly(I:C) is associated with higher TLR3 stimulation rather than with the activation of different receptors, we first verified to what extent poly(I:C) encapsulation by Lipofectamine improves its uptake by PC3 and DU145 cells. For this purpose, both cell lines were treated with rhodamine-labeled ex-poly(I:C), alone at 25 μg/ml, or with in-poly(I:C) at 2 μg/ml and then subjected to flow cytometric analysis. Strikingly, after 6 h of in-poly(I:C) treatment, the mean of rhodamine fluorescence rose up to about 60 compared with 10 after ex-poly(I:C) at 25 μg/ml, indicating a 6-fold increase in poly(I:C) uptake by transfection compared with a 12-fold higher dosage of ex-poly(I:C) (Fig. 4*A*). Subsequently, in order to assess if in-poly(I:C) comes into contact with endosomes, we performed confocal laser-scanning microscopy experiments in PC3 cells treated with rhodamine-labeled poly(I:C), alone or in combination with Lipofectamine, in the presence of GFP-labeled early endosome marker (fluorescent protein signal peptide targeting Rab5a). Interestingly, despite poly(I:C)/endosome co-localization after both treatments, in-poly(I:C) was localized in early endosomes with much more efficiency even than ex-poly(I:C) at 25 μg/ml (Fig. 4*B*). To quantify the amount of colocalization between the red and green signals at different times of treatment, we used Manders' correlation coefficient (Fig. 4*C*), which suggests a high and similar colocalization under all conditions, despite the different timing and fluorescence intensities upon different treatments. Moreover, there is no significant co-localization of in-poly(I:C) with the late endosome marker Rab7a (data not shown).

IRF3 and IFN-β Are Implicated in RLH Up-regulation but Not in Apoptosis Induced by Transfected Poly(I:C)—After demonstrating the key role of TLR3 in in-poly(I:C)-induced apoptosis, we analyzed its downstream pathways. TLR3 engagement by ligand triggers the activation of IRF3, leading to induction of type I IFNs and other inflammatory cytokines (17). IRF3 mediates cytotoxic activity of poly(I:C)-cationic liposome LIC-101 complex against HeLa cells (34). In the present work, we hypothesized the involvement of IRF3 in TLR3-mediated apoptosis also in PC3 and DU145 cells. We first evaluated IRF3 activation assayed by detection of phosphorylated IRF3. As shown in Fig. 5*A*, IRF3 phosphorylation increases after in-poly(I:C) in a time-dependent manner in both cell lines. To investigate the role of IRF3 activation in apoptosis, we first used BX795, a pharmacological inhibitor of TBK1/IKK-ϵ, to inhibit IRF3 phosphorylation induced by in-poly(I:C) (Fig. 5*B*). PC3 and DU145 cells were treated with in-poly(I:C) alone and in combination with BX795, and then cells were subjected to cell cycle analysis after PI incorporation. As shown in Fig. 5*C*, in-

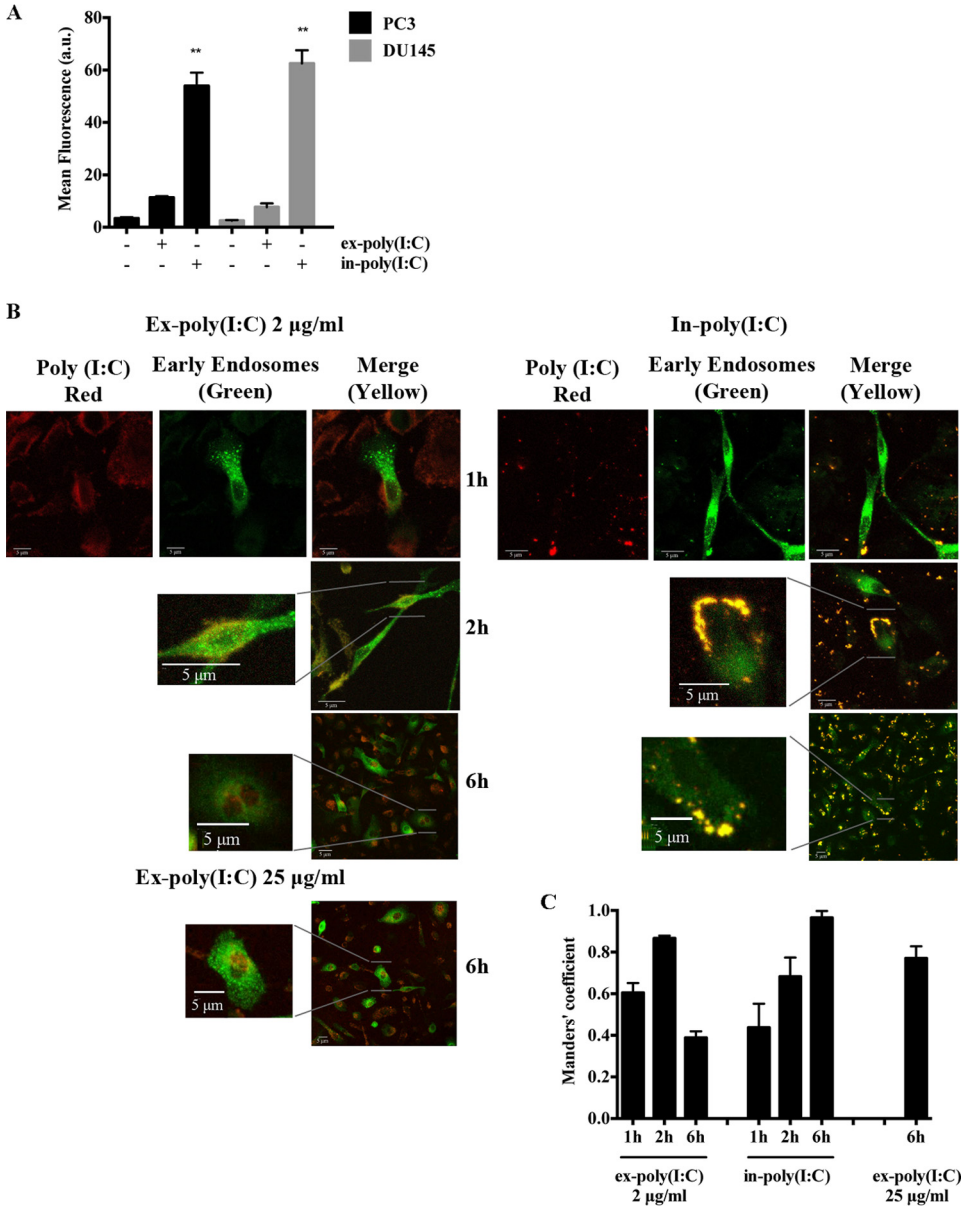

FIGURE 4. **Enhancement of poly(I:C) uptake in PC3 and DU145 cells by transfection and in-poly(I:C) co-localization with early endosomes.** *A*, PC3 and DU145 cells were treated with in-poly(I:C)-rhodamine or ex-poly(I:C)-rhodamine labeled for 6 h and then subjected to flow cytometry analysis to evaluate the fluorescence intensity of rhodamine-positive cells. Results are presented as mean ± range. *a.u.*, arbitrary units. *B*, confocal laser-scanning microscopy of PC3 cells treated with rhodamine-labeled poly(I:C) at 2 μg/ml plus Lipofectamine (in-poly(I:C)) or rhodamine-labeled ex-poly(I:C) (25 or 2 μg/ml) at the indicated times in the presence of GFP-labeled early endosomes marker Rab5a. Images are representative of three independent experiments. *C*, the histograms represent Manders' coefficient measured as the amount of fluorescence of the co-localizing objects in each component, which is dependent on the intensities of the signals ($n = 5$ or 10 cells/experiment). *Error bars*, S.D.

poly(I:C)-induced apoptosis was not inhibited in the presence of BX795. This finding was confirmed after IRF3-specific down-regulation by siRNA (Fig. 5*D*), demonstrating that IRF3 is not implicated in in-poly(I:C)-induced apoptosis in PC3 and DU145 cell lines. Because it has been reported that the phosphorylation site at Ser-396 of the IRF3 regulatory domain is directly targeted by IKK-ϵ (35), we used the IKK-ϵ kinase inhibitor II, a benzimidazole analog. This molecule acts as a selective inhibitor of IKK-ϵ kinase and allows us to discriminate the role of TBK1 and IKK-ϵ in IRF3 phosphorylation and in in-poly(I:C)-induced apoptosis. Data in Fig. 5*E* show that IRF3 phosphorylation was abolished by IKK-ϵ, whereas in-poly(I:C)-induced apoptosis was completely unaffected (Fig. 5*F*).

Phosphorylated IRF3 becomes active and translocates to the nucleus, where it operates as a transcriptional factor inducing antiviral genes as type I IFNs, which are also critical regulators of NK cell activation and have antitumor activity (36). In this regard, to confirm the canonical role of IRF3 in IFN type I induction, we transfected PC3 cells with a plasmid containing luciferase under the IFN-β promoter and assayed the luciferase activity after poly(I:C) alone and in combination with the IRF3 inhibitor BX795 for 3 h. DU145 cells were not tested because they have been described as not being able to produce IFN type I after poly(I:C) treatment (20). The pretreatment with BX795 abrogates the induction of IFN-β transcription, demonstrating the key role of IRF3 in the activation of the IFN-β promoter

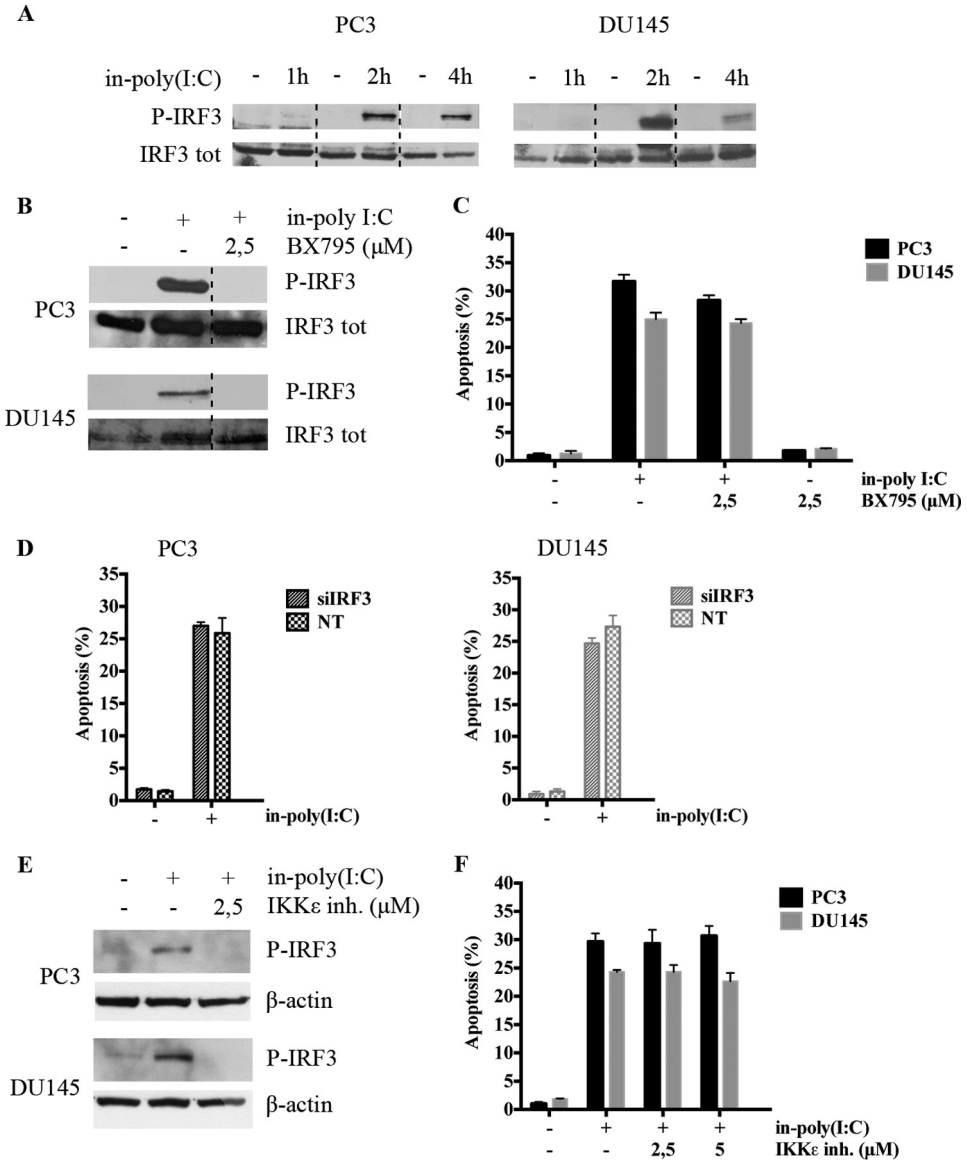

FIGURE 5. **IKK-ϵ-dependent IRF3 activation is not implicated in apoptosis induced by transfected poly(I:C) in both cell lines.** *A*, Western blot analysis of phosphorylated IRF3 (*P-IRF3*) of whole cell lysates obtained from PC3 and DU145 cells after in-poly(I:C) treatment at the indicated times. Data were normalized against total IRF3. *B*, PC3 and DU145 cells were treated with in-poly(I:C) alone or in combination with BX795, and then cell lysates were subjected to Western blot analysis to confirm phospho-IRF3 inhibition. Data were normalized against total IRF3. *C*, PI staining of PC3 and DU145 cells after 48 h of treatment with in-poly(I:C) alone or in combination with BX795. The histograms represent the mean ± S.D. (*error bars*) of the apoptotic cell percentage obtained in three independent experiments. *D*, PC3 and DU145 cells were treated with siRNA specific for IRF3 (*siIRF3*) or with control siRNA (*NT*) for 72 h. Cells were treated with in-poly(I:C) for 48 h and then subjected to cell cycle analysis after PI incorporation. The histograms represent the mean ± S.D. of the percentage of apoptotic cells of three independent experiments. The differences between NT and siIRF3 are not significant. *E*, PC3 and DU145 cells were treated with in-poly(I:C) alone or in combination with IKK-ϵ kinase inhibitor, and then whole cell lysates were subjected to Western blot analysis to confirm phospho-IRF3 inhibition. Data were normalized against β-actin. *F*, PI staining of PC3 and DU145 cells after 48 h of treatment with in-poly(I:C) alone or in combination with IKK-ϵ kinase inhibitor (*inh.*). The histograms represent the mean ± S.D. of the apoptotic cell percentage obtained in three independent experiments. Data in *A*, *B*, and *E* are representative of three Western blots from three independent experiments.

(Fig. 6*A*). Moreover, we analyzed whether IRF3 was involved in in-poly(I:C)-induced up-regulation of MDA5, RIG-I, and TLR3. To this purpose, PC3 and DU145 cells were treated with in-poly(I:C) alone or combined with BX795 and then subjected to Western blot analysis for the evaluation of expression of the three dsRNA receptors. Fig. 6*B* shows that IRF3 inhibition abolished the up-regulation of MDA5, RIG-I, and TLR3. To clarify which receptor(s) trigger IRF3 activation in our models, we performed Western blot analysis for phospho-IRF3 in PC3 and DU145 cells that had undergone siRNA-mediated MDA5 and RIG-I knockdown. MDA5 siRNA abrogated IRF3 phosphorylation upon in-poly(I:C) stimulation in both cell lines (Fig. 6*C*), whereas nonfunctional RIG-I impaired IRF3 phosphorylation only in DU145 cells (Fig. 6*D*), suggesting that MDA5 alone or together with RIG-I transduces through IRF3, which in turn triggers IFN-β production.

After demonstrating that in-poly(I:C)-apoptosis is IRF3-independent but is accompanied by IFN-β increased expression, we evaluated whether IFN-β mediates in an autocrine fashion in-poly(I:C)-triggered apoptosis, as described previously in different cancer cell lines (2, 37, 38). With this aim, we blocked type I interferon receptor (IFNR-1) by a neutralizing antibody,

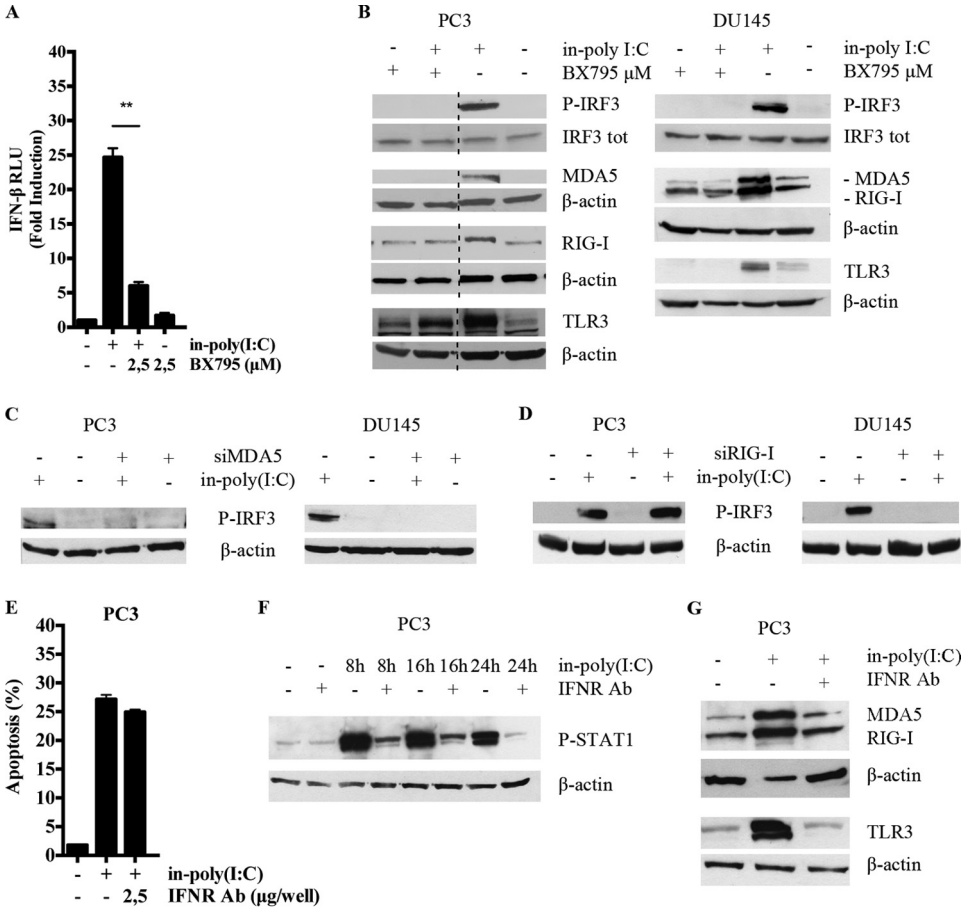

FIGURE 6. **IRF3 is implicated in the induction of interferon-β, MDA5, RIG-I, and TLR3 expression.** *A*, PC3 cells transiently transfected with IFNβ-pGL3-luc plasmid were treated with in-poly(I:C) alone or in combination with BX795 for 3 h and then subjected to a luciferase assay. Interferon-β expression was assayed by using the p-IFNβ-pGL3 luciferase reporter described under "Experimental Procedures." The histograms represent the -fold induction of IFN expression calculated from the mean ± S.D. (*error bars*) of luciferase intensity obtained in three independent experiments. The exact *p* values are reported *versus* respective controls (Student's paired *t* test): **, $p < 0.01$. *B*, Western blot analysis for phospho-IRF3, MDA5, RIG-I, and TLR3 of whole cell lysates obtained from PC3 and DU145 cells treated with in-poly(I:C) alone or in combination with BX795 for 24 h. *C* and *D*, Western blot analysis for phosphorylated IRF3 (*P-IRF3*) of cell lysates obtained from PC3 and DU145 cells treated with in-poly(I:C) after MDA5/RIG-I siRNAs or scrambled siRNA (−). *E*, PI staining of PC3 cells treated with in-poly(I:C) alone or in combination with IFNR-neutralizing antibody (*IFNR Ab*) for 48 h. The histograms represent the mean ± S.D. of the percentage of apoptotic cells obtained in three independent experiments. *F*, time course analysis of phosphorylated STAT1 (*P-STAT1*) assessed by Western blot of whole cell lysates from PC3 cells treated with in-poly(I:C) alone or in combination with IFNR-neutralizing antibody. *G*, Western blot analysis for MDA5, RIG-I, and TLR3 of whole cell lysates obtained from PC3 cells treated with in-poly(I:C) alone or in combination with IFNR-neutralizing antibody for 24 h. Data in *B*, *C*, *D*, *F*, and *G* were normalized against β-actin and are representative of three Western blots from three independent experiments.

and we assessed apoptosis rate after in-poly(I:C) treatment in PC3 cells. Fig. 6*E* shows no effect of IFNR-1 on in-poly(I:C)-induced apoptosis. The inhibitory effect of the antibody was tested by evaluating STAT1 phosphorylation, which is a downstream signal of type I IFNR activation. STAT1 phosphorylation following in-poly(I:C) stimulation was inhibited by IFNR-neutralizing antibody, confirming the functionality of the antibody (Fig. 6*F*). As described in various cell types, type I interferons produced upon poly(I:C) stimulation can act in an autocrine manner, thereby increasing dsRNA receptor expression (39). To test this possibility in PC3 cells, we assessed dsRNA receptor protein levels after in-poly(I:C) treatment in combination with IFNR-neutralizing antibody. Fig. 6*G* shows that the up-regulation of MDA5, RIG-I, and TLR3 induced by in poly(I:C) was abolished in IFNR knockdown conditions.

Signaling Pathways Implicated in Apoptosis Induced by Transfected Poly(I:C)—After excluding the involvement of IFN-β in mediating in-poly(I:C)-triggered apoptosis in PC3 cells, we investigated the pathways directly activated by poly(I:C) transfection. TLR3 stimulation triggers activation of MAPKs (17). We then investigated the role of MAPKs in in-poly(I:C)-induced apoptosis because we have previously demonstrated their role in apoptosis induced by TLR3-dependent ex-poly(I:C) (18). With this purpose, we first evaluated JNK and p38 activation after in-poly(I:C) treatment. As shown in Fig. 7*A*, in-poly(I:C) stimulation induces activation of JNK and p38 in a time-dependent manner in both cell lines. Afterward, to evaluate their implication in apoptosis, we used the specific pharmacological inhibitors SP600125 for JNK and SB203580 for p38. Cells were subjected to cell cycle analysis after PI incorporation, and the histograms in Fig. 7*B* demonstrate that the apoptotic rate induced by in-poly(I:C) was strongly reduced in the presence of JNK and/or p38 inhibitors in both cell lines, demonstrating their essential role in the apoptotic pathway. By using stably transfected DN-TLR3 PC3 cells and Pepinh-TRIF-treated DU145 cells, we observed a significant inhibition of in-poly(I:C)-induced JNK and p38 phosphorylation in transfected DN-TLR3 PC3 cells *versus* P-PURO-PC3 cells and Pepinh-

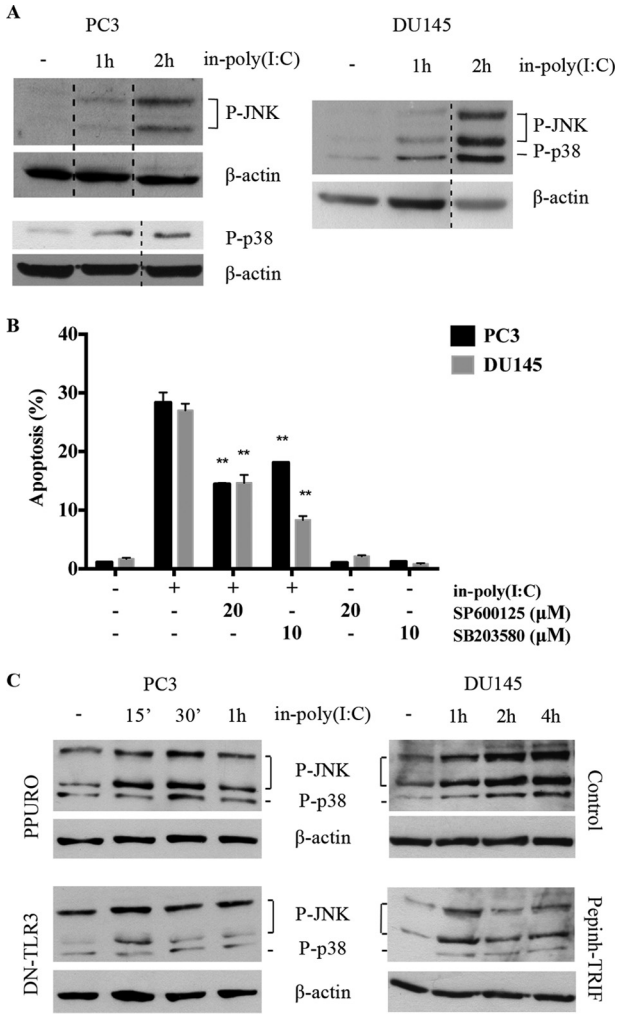

FIGURE 7. **JNK and p38 are implicated in in-poly(I:C)-induced apoptosis.** *A*, Western blot analysis of phosphorylated JNK (*P-JNK*) and p38 (*P-p38*) of PC3 and DU145 cell lysates after in-poly(I:C) treatment at the indicated times. Data were normalized against β-actin. *B*, apoptosis assayed by PI staining of PC3 and DU145 cells after in-poly(I:C) treatment alone or in combination with JNK inhibitor (SP600125) or p38 inhibitor (SB203580), as indicated. The histograms represent the mean ± S.D. (*error bars*) of the percentage of apoptotic cells of three independent experiments. The exact *p* values are reported *versus* the respective controls (Student's paired *t* test): **, $p < 0.01$. *C*, Western blot analysis after in-poly(I:C) treatment for phosphorylated JNK and p38 in whole cell lysates obtained from DN-TLR3 PC3 cells and DU145 cells pretreated with Pepinh-TRIF and the respective controls. Data were normalized against β-actin. Data in *A* and *C* are representative of three Western blots from three independent experiments.

TRIF-treated DU145 cells *versus* control DU145 cells in both PCa cell lines (Fig. 7*C*).

Src and STAT1 Involvement in TLR3-dependent Apoptotic Signaling—It has been demonstrated that TLR3 signaling involves the proto-oncoprotein Src, which plays an essential role for dsRNA-elicited STAT1 and IRF3 activation (10). To investigate the role of Src in in-poly(I:C)-induced apoptosis, PC3 and DU145 cells were pretreated with the specific Src pharmacological inhibitor SU6656, prior to in-poly(I:C) stimulation. In both cell lines, apoptosis was markedly decreased in the presence of in-poly(I:C) plus SU6656 (Fig. 8*A*). Therefore, we assayed STAT1 phosphorylation following in-poly(I:C) treatment. Data in Fig. 8*B* show that STAT1 was rapidly activated, starting from 15 min after in-poly(I:C) stimulation in both cell lines, and that its phosphorylation was more extended in DU145 cells than in PC3 cells. SU6656 completely reverted STAT1 activation in both cell lines. Interestingly, IRF3 phosphorylation induced by in-poly(I:C) is not affected by SU6656 (Fig. 8*C*). In order to evaluate whether Src also influences JNK and p38 activation, we tested SU6656 on JNK and p38 phosphorylation. As shown in Fig. 8*D*, Src inhibition does not decrease JNK and p38 activation, demonstrating that MAPK and Src/STAT1 activation take place through separate signaling pathways.

In summary, the data obtained in the present work highlight distinct pathways triggered by in-poly(I:C) in two androgen-resistant PCa cell lines: one mediated by TLR3, leading to apoptosis in an IRF3-independent fashion, and the other one TLR3-independent, mediated by the cytosolic receptors MDA5 and RIG-I, IRF3-dependent, and leading to IFN-β production. Moreover IFN-β, although it is up-regulated, does not influence in-poly(I:C)-induced apoptosis.

DISCUSSION

In this study, we report that dsRNA transfection in the most aggressive androgen-independent prostate cancer cell lines, PC3 and DU145, exerts an antitumor effect by eliciting different responses mediated by distinct receptors and transduction pathways: apoptosis, via TLR3, and IRF3-dependent IFN-β-mediated immunoadjuvant response, via MDA5 in PC3 cells and via MDA5 and RIGI in DU-145 cells. IFN-β is known to be a key molecule in antitumoral immune response in various cancers, including PCa (40, 41). Moreover, in different cancer models, IFN-β has been shown to mediate poly(I:C)-dependent apoptosis or growth arrest (2, 37, 38). In contrast, in this work, by using neutralizing antibody against IFNR, we demonstrate that in-poly(I:C)-induced apoptosis takes place independently of IFN-β in androgen-independent PCa cells. The present data are also in agreement with our previous work (18) showing that ex-poly(I:C) induces apoptosis in a TLR3-dependent fashion independently of IFN-β in the androgen-dependent LNCaP cell line, which is IFN-insensitive. Here we show that in-poly(I:C) is able to directly trigger apoptosis by a rapid and transient induction of Src-dependent STAT1 activation, indicating that in-poly(I:C) directly activates STAT1, independently from IFN-β, which is produced afterward. Our data are consistent with those of Dempoya *et al.* (42), who reported a poly(I:C)-induced STAT1 phosphorylation in both a type I IFN-dependent manner and a type I IFN-independent manner, depending on the period of time after the introduction of poly(I:C) into the cells.

So far, only dsRNA cytosolic receptors have been implicated in the apoptotic effect induced by transfected poly(I:C) or viral dsRNA in prostate, gastric, breast, and melanoma cancers (20, 43–45). The most specific cytosolic receptor for poly(I:C) was demonstrated to be MDA5 (46), which mainly mediates antitumor effects (45). Surprisingly, we found that MDA5 does not contribute to in-poly(I:C)-induced apoptosis. Accordingly, Myksiw *et al.* (47) have shown that RNA species produced during virus replication induce the activation of apoptosis in a PKR-dependent but MDA5- and RIG-I-independent fashion. With regard to prostate cancer, in particular, it has been dem-

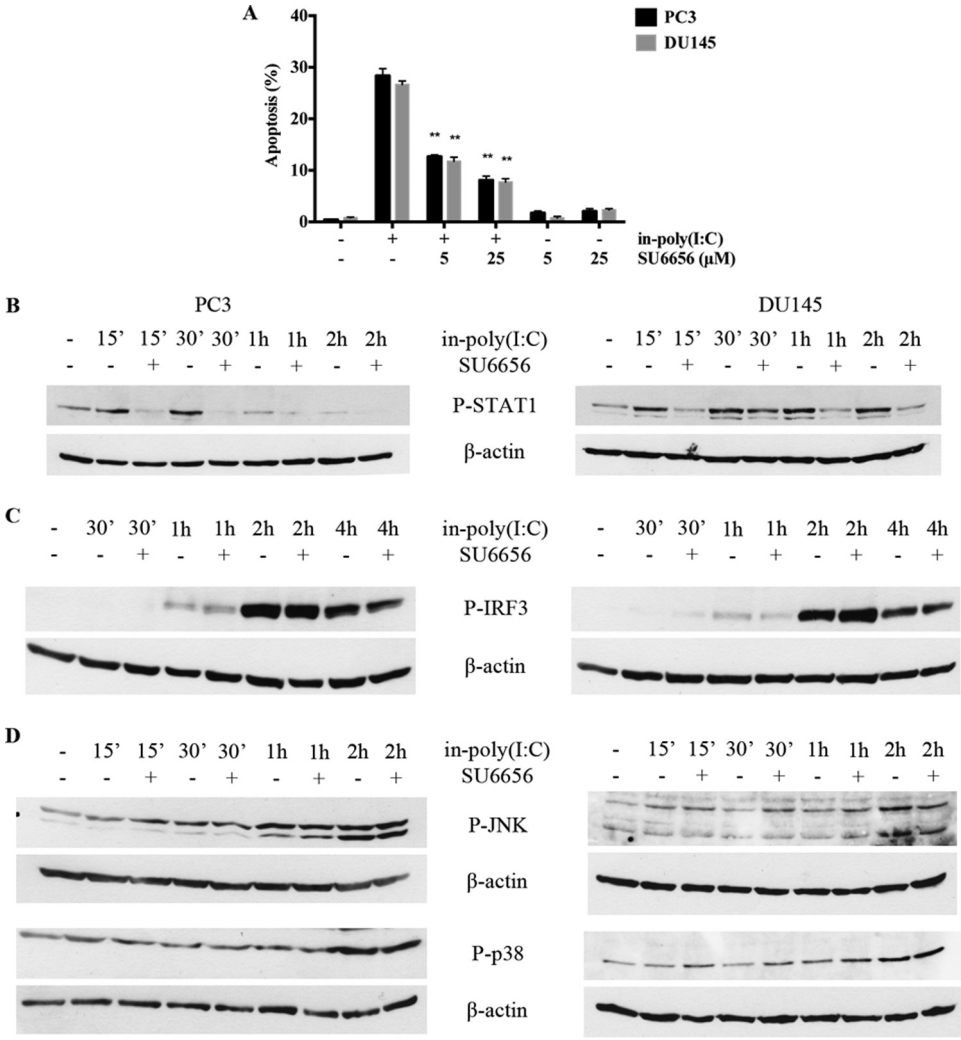

FIGURE 8. **Implication of Src and STAT1 in apoptosis induced by in-poly(I:C).** *A*, PI staining of PC3 and DU145 cells after 48 h of treatment with in-poly(I:C) alone or in combination with Src inhibitor (SU66656). The histograms represent the mean ± S.D. of apoptotic cells obtained in three independent experiments. The exact *p* values are reported *versus* respective controls (Student's paired *t* test): **, $p < 0.01$. *B–D*, Western blot analysis of whole cell lysates obtained from PC3 and DU145 cells of the indicated phosphoproteins after the in-poly(I:C) with or without SU66656 treatments for different times. Data were normalized against β-actin. Data in *B–D* are representative of three Western blots from three independent experiments.

onstrated that an intracellular viral RNA genome from hemagglutinating virus of Japan suppressed the viability of PC3 and DU145 cells with two different mechanisms, Trail- and IRF3-dependent in PC3 cells and Noxa- and IRF-7-dependent in DU145 cells, both downstream of cytoplasmic RNA receptor RIG-I (20). Conversely, in the present paper, by using knockdown by siRNA or specific pharmacological inhibition of PKR, MDA5, RIG-I, and MAVS, we excluded the involvement of all cytosolic receptors in in-poly(I:C)-induced apoptosis. In agreement, we have recently encapsulated poly(I:C) with three cationic liposome formulations with comparable levels in cell uptake in endocytic vesicles but distinct tendencies to release gene cargo in the cytosol, and we observed that the release of poly(I:C) in the cytosol seems not to be critical for induction of apoptosis in PC3 and DU145 cells (21). In the present study, we demonstrate, by co-immunolocalization and FACS assays, that endocytosis was the major mechanism of delivery for in-poly(I:C), which, at the lowest dose, induces a strong enhancement in cellular uptake when compared with a 12-fold higher concentration of ex-poly(I:C). Because we observed a marked decrease of cell viability of PC3 and DU145 cells after in-poly(I:C) compared with ex-poly(I:C), we demonstrated that the relevant endocytic uptake can greatly favor poly(I:C) binding to endosomal TLR3, consequently promoting high levels of apoptosis. By using a dominant negative TLR3, we show that TLR3 is crucial for in-poly(I:C)-induced apoptosis compared with poly(I:C) interaction with cytosolic receptors, suggesting that the highly efficient poly(I:C) localization in the endosomes after in-poly(I:C) as compared with ex-poly(I:C) accounts for the strong apoptotic effect due to the induction of caspase-9 activity, absent after ex-poly(I:C), and higher caspase-8 activity after in-poly(I:C) than after ex-poly(I:C) in both PCa cell lines.

Thereafter, we focused our attention on identifying the signaling pathways responsible for in-poly(I:C)-induced apoptosis. The role of the Src pathway downstream of growth factors is well known. In fact, Src involvement in PDGF- and EGF-mediated tyrosine phosphorylation of STAT1 and STAT3 has been reported in tumor and normal cells with different biological activity (48, 49). In this report, we show for the first time the involvement of the TLR3/Src/STAT1 pathway in mediating in-

poly(I:C)-induced apoptosis. In fact, Src inhibition blocks apoptosis concurrently with the inhibition of STAT1 activation but does not affect IRF3 phosphorylation, in agreement with the notion that in our model IRF3 is downstream of the MDA5/RIGI pathways and is not involved in apoptosis. Interestingly, it has been demonstrated that the tyrosine kinase Src is activated also by extracellular dsRNA, which triggers its association with TLR3 essential for dsRNA-elicited IRF3 and STAT1 activation (10, 50).

Moreover, by using MAPK-specific inhibitors and TLR3 knockdown cells, we observed that p38 and JNK MAPK pathways controlled TLR3-mediated cell death in PC3 and DU145 cells upon in-poly(I:C) stimulation. Accordingly, a role for p38 has been demonstrated also in TLR2-dependent apoptosis (51), and inhibition of p38 MAPK activity alleviates apoptosis induced by Japanese encephalitis virus (52). In regard to the interaction between the MAPK and Src pathways in our model, our data show that the inhibition of Src does not affect JNK and p38 activation, in agreement with Johnsen *et al.* (10), who showed that MAPK activation in response to dsRNA occurs through separate signaling pathways that diverge upstream of Src.

Besides its key role in antiviral immunity, IRF3 activation by virus infection is essential for triggering a direct apoptotic response, as manifested by the fact that infected cells are not killed in the absence of IRF3 and become persistently infected (53–55). In agreement, we have recently demonstrated that IRF3 mediates apoptosis in response to dsRNA in androgen-sensitive PCa cells (56) as well as, as previously observed, in melanoma and fibrosarcoma cells (57). Conversely, in this work, we found that in-poly(I:C)-induced apoptosis is completely independent of IRF3, as shown by using genetic and pharmacological approaches. In our model, IRF3 is involved exclusively in MDA5- and RIG-I-dependent up-regulation of IFN-β, which in turn accounts for MDA5, RIG-I, and TLR3 protein increase. This demonstrates that IRF3-mediated IFN-β production is dependent on an intact MDA5/RIGI/MAVS/IRF3 axis, but, at least in PC3 cells that express type I IFN receptor, the subsequent expansion of antiviral/immunoadjuvant response is driven by the binding of newly synthesized IFN-β on its receptor, which acts in an autocrine fashion to up-regulate the expression of interferon-stimulated genes, such as all of the dsRNA receptors, as reviewed previously (39). Further, MDA5 expression was shown to be virus-inducible in cells lacking the IFN receptor, suggesting that RLH expression could be driven by a direct virus-inducible signal (58). Accordingly, we found an IRF3-dependent increase of dsRNA receptors after in-poly(I:C) in DU145 cells, although they do not express the type I interferon receptor. Recently, Zhou *et al.* (59) reported that in different cell lines, the activation of TLR3 leading to IFN production can be triggered either by naked poly(I:C) or only by transfected poly(I:C). In agreement, our data enforce the notion that the delivery of poly(I:C) is a key factor in influencing specific antiviral responses according to the target cell type.

Collectively, our data show two different in-poly(I:C)-activated tumor suppressor pathways leading to apoptosis and to the production of antiviral/immunoadjuvant molecules. Because many of the efforts regarding anti-cancer drug development employ encapsulation of antitumor drugs in order to reduce the drug dosage required (60), our data may be of clinical relevance in order to target tumor cells both by inducing apoptosis and by immunologically mediated antitumor responses.

REFERENCES

1. Shen, M. M., and Abate-Shen, C. (2010) Molecular genetics of prostate cancer: new prospects for old challenges. *Genes Dev.* **24,** 1967–2000
2. Salaun, B., Coste, I., Rissoan, M. C., Lebecque, S. J., and Renno, T. (2006) TLR3 can directly trigger apoptosis in human cancer cells. *J. Immunol.* **176,** 4894–4901
3. Akira, S., and Takeda, K. (2004) Toll-like receptor signaling. *Nat. Rev. Immunol.* **4,** 499–511
4. Vacchelli, E., Martins, I., Eggermont, A., Fridman, W. H., Galon, J., Sautès-Fridman, C., Tartour, E., Zitvogel, L., Kroemer, G., and Galluzzi, L. (2012) Trial watch: peptide vaccines in cancer therapy. *Oncoimmunology* **1,** 1557–1576
5. Cheng, Y. S., and Xu, F. (2010) Anticancer function of polyinosinic-polycytidylic acid. *Cancer Biol. Ther.* **10,** 1219–1223
6. Alexopoulou, L., Holt, A. C., Medzhitov, R., and Flavell, R. A. (2001) Recognition of double-stranded RNA and activation of NF-κB by Toll-like receptor 3. *Nature* **413,** 732–738
7. Yamamoto, M., Sato, S., Hemmi, H., Hoshino, K., Kaisho, T., Sanjo, H., Takeuchi, O., Sugiyama, M., Okabe, M., Takeda, K., and Akira, S. (2003) Role of adaptor TRIF in the MyD88-independent toll-like receptor signaling pathway. *Science* **301,** 640–643
8. Fitzgerald, K. A., McWhirter, S. M., Faia, K. L., Rowe, D. C., Latz, E., Golenbock, D. T., Coyle, A. J., Liao, S. M., and Maniatis, T. (2003) IKKϵ and TBK1 are essential components of the IRF3 signaling pathway. *Nat. Immunol.* **4,** 491–496
9. Doyle, S., Vaidya, S., O'Connell, R., Dadgostar, H., Dempsey, P., Wu, T., Rao, G., Sun, R., Haberland, M., Modlin, R., and Cheng, G. (2002) IRF3 mediates a TLR3/TLR4-specific antiviral gene program. *Immunity* **17,** 251–263
10. Johnsen, I. B., Nguyen, T. T., Ringdal, M., Tryggestad, A. M., Bakke, O., Lien, E., Espevik, T., and Anthonsen, M. W. (2006) Toll-like receptor 3 associates with c-Src tyrosine kinase on endosomes to initiate antiviral signaling. *EMBO J.* **25,** 3335–3346
11. Yoneyama, M., Kikuchi, M., Natsukawa, T., Shinobu, N., Imaizumi, T., Miyagishi, M., Taira, K., Akira, S., and Fujita, T. (2004) The RNA helicase RIG-I has an essential function in double-stranded RNA-induced innate antiviral responses. *Nat. Immunol.* **5,** 730–737
12. Kato, H., Takeuchi, O., Sato, S., Yoneyama, M., Yamamoto, M., Matsui, K., Uematsu, S., Jung, A., Kawai, T., Ishii, K. J., Yamaguchi, O., Otsu, K., Tsujimura, T., Koh, C. S., Reis e Sousa, C., Matsuura, Y., Fujita, T., and Akira, S. (2006) Differential roles of MDA5 and RIG-I helicases in the recognition of RNA viruses. *Nature* **441,** 101–105
13. Kawai, T., Takahashi, K., Sato, S., Coban, C., Kumar, H., Kato, H., Ishii, K. J., Takeuchi, O., and Akira, S. (2005) IPS-1, an adaptor triggering RIG-I and MDA5-mediated type I interferon induction. *Nat. Immunol.* **6,** 981–988
14. Meylan, E., Curran, J., Hofmann, K., Moradpour, D., Binder, M., Bartenschlager, R., and Tschopp, J. (2005) Cardif is an adaptor protein in the RIG-I antiviral pathway and is targeted by hepatitis C virus. *Nature* **437,** 1167–1172
15. Seth, R. B., Sun, L., Ea, C. K., and Chen, Z. J. (2005) Identification and characterization of MAVS, a mitochondrial antiviral signaling protein that activates NF-κB and IRF3. *Cell* **122,** 669–682
16. Xu, L. G., Wang, Y. Y., Han, K. J., Li, L. Y., Zhai, Z., and Shu, H. B. (2005) VISA is an adapter protein required for virus-triggered IFN-β signaling. *Mol. Cell* **19,** 727–740
17. Kawai, T., and Akira, S. (2006) Innate immune recognition of viral infection. *Nat. Immunol.* **7,** 131–137
18. Paone, A., Starace, D., Galli, R., Padula, F., De Cesaris, P., Filippini, A., Ziparo, E., and Riccioli, A. (2008) Toll-like receptor 3 triggers apoptosis of human prostate cancer cells through a PKC-α-dependent mechanism.

Carcinogenesis **29,** 1334–1342
19. Galli, R., Paone, A., Fabbri, M., Zanesi, N., Calore, F., Cascione, L., Acunzo, M., Stoppacciaro, A., Tubaro, A., Lovat, F., Gasparini, P., Fadda, P., Alder, H., Volinia, S., Filippini, A., Ziparo, E., Riccioli, A., and Croce, C. M. (2013) Toll-like receptor 3 (TLR3) activation induces microRNA-dependent re-expression of functional RARβ and tumor regression. *Proc. Natl Acad. Sci. U.S.A.* **110,** 9812–9817
20. Matsushima-Miyagi, T., Hatano, K., Nomura, M., Li-Wen, L., Nishikawa, T., Saga, K., Shimbo, T., and Kaneda, Y. (2012) TRAIL and Noxa are selectively upregulated in prostate cancer cells downstream of the RIG-I/MAVS signaling pathway by nonreplicating Sendai virus particles. *Clin. Cancer Res.* **18,** 6271–6283
21. Palchetti, S., Pozzi, D., Riccioli, A., Ziparo, E., Colapicchioni, V., Amenitsch, H., and Caracciolo, G. (2013) Structural characterization of cationic liposome/poly(I:C) complexes showing high ability in eliminating prostate cancer cells. *RSC Adv.* 10.1039/C3RA44093A
22. Mosmann, T. (1983) Rapid colorimetric assay for cellular growth and survival: application to proliferation and cytotoxicity assays. *J. Immunol. Methods* **65,** 55–63
23. Paone, A., Galli, R., Gabellini, C., Lukashev, D., Starace, D., Gorlach, A., De Cesaris, P., Ziparo, E., Del Bufalo, D., Sitkovsky, M. V., Filippini, A., and Riccioli, A. (2010) Toll-like receptor 3 regulates angiogenesis and apoptosis in prostate cancer cell lines through hypoxia-inducible factor 1α. *Neoplasia* **12,** 539–549
24. Lin, R., Génin, P., Mamane, Y., and Hiscott, J. (2000) Selective DNA binding and association with the CREB binding protein coactivator contribute to differential activation of α/β interferon genes by interferon regulatory factors 3 and 7. *Mol. Cell. Biol.* **20,** 6342–6353
25. Manders, E. M. M., Verbeek, F. J., and Aten, J. A. (1993) Measurement of co-localization of objects in dual-colour confocal images. *J. Microsc.* 10.1111/j.1365–2818.1993.tb03313.x
26. Faraji, A. H., and Wipf, P. (2009) Nanoparticles in cellular drug delivery. *Bioorg. Med. Chem.* **17,** 2950–2962
27. Hirabayashi, K., Yano, J., Inoue, T., Yamaguchi, T., Tanigawara, K., Smyth, G. E., Ishiyama, K., Ohgi, T., Kimura, K., and Irimura, T. (1999) Inhibition of cancer cell growth by polyinosinic-polycytidylic acid/cationic liposome complex: a new biological activity. *Cancer Res.* **59,** 4325–4333
28. Peng, S., Geng, J., Sun, R., Tian, Z., and Wei, H. (2009) Polyinosinic-polycytidylic acid liposome induces human hepatoma cells apoptosis which correlates to the up-regulation of RIG-I like receptors. *Cancer Sci.* **100,** 529–536
29. Chen, M., and Wang, J. (2002) Initiator caspases in apoptosis signaling pathways. *Apoptosis* **7,** 313–319
30. Gil, J., Alcamí, J., and Esteban, M. (1999) Induction of apoptosis by double-stranded-RNA-dependent protein kinase (PKR) involves the α subunit of eukaryotic translation initiation factor 2 and NF-κB. *Mol. Cell. Biol.* **19,** 4653–46663
31. Meylan, E., Tschopp, J., and Karin, M. (2006) Intracellular pattern recognition receptors in the host response. *Nature* **442,** 39–44
32. Alonso-Curbelo, D., and Soengas, M. S. (2010) Self-killing of melanoma cells by cytosolic delivery of dsRNA: wiring innate immunity for a coordinated mobilization of endosomes, autophagosomes and the apoptotic machinery in tumor cells. *Autophagy* **6,** 148–150
33. Le Blanc, I., Luyet, P. P., Pons, V., Ferguson, C., Emans, N., Petiot, A., Mayran, N., Demaurex, N., Fauré, J., Sadoul, R., Parton, R. G., and Gruenberg, J. (2005) Endosome-to-cytosol transport of viral nucleocapsids. *Nat. Cell Biol.* **7,** 653–664
34. Uno, T., Hirabayashi, K., Murai, M., Yano, J., and Ozato, K. (2005) The role of IFN regulatory factor-3 in the cytotoxic activity of NS-9, a polyinosinic-polycytidylic acid/cationic liposome complex, against tumor cells. *Mol. Cancer Ther.* **4,** 799–805
35. Fujii, K., Nakamura, S., Takahashi, K., and Inagaki, F. (2010) Systematic characterization by mass spectrometric analysis of phosphorylation sites in IRF-3 regulatory domain activated by IKK-i. *J. Proteomics* **73,** 1196–1203
36. Hertzog, P. J., and Williams, B. R. (2013) Fine tuning type I interferon responses. *Cytokine Growth Factor Rev.* **24,** 217–225
37. Van, D. N., Roberts, C. F., Marion, J. D., Lépine, S., Harikumar, K. B., Schreiter, J., Dumur, C. I., Fang, X., Spiegel, S., and Bell, J. K. (2012) Innate immune agonist, dsRNA, induces apoptosis in ovarian cancer cells and enhances the potency of cytotoxic chemotherapeutics. *FASEB J.* **26,** 3188–3198
38. Harashima, N., Minami, T., Uemura, H., and Harada, M. (2014) Transfection of poly(I:C) can induce reactive oxygen species-triggered apoptosis and interferon-β-mediated growth arrest in human renal cell carcinoma cells via innate adjuvant receptors and the 2-5A system. *Mol. Cancer* **13,** 217–229
39. Goubau, D., Deddouche, S., and Reis e Sousa, C. (2013) Cytosolic sensing of viruses. *Immunity* **38,** 855–869
40. Chin, A. I., Miyahira, A. K., Covarrubias, A., Teague, J., Guo, B., Dempsey, P. W., and Cheng, G. (2010) Toll-like receptor 3-mediated suppression of TRAMP prostate cancer shows the critical role of type I interferons in tumor immune surveillance. *Cancer Res.* **70,** 2595–2603
41. Gatti, G., Nuñez, N. G., Nocera, D. A., Dejager, L., Libert, C., Giraudo, C., and Maccioni, M. (2013) Direct effect of dsRNA mimetics on cancer cells induces endogenous IFN-β production capable of improving dendritic cell function. *Eur. J. Immunol.* **43,** 1849–1861
42. Dempoya, J., Matsumiya, T., Imaizumi, T., Hayakari, R., Xing, F., Yoshida, H., Okumura, K., and Satoh, K. (2012) Double-stranded RNA induces biphasic STAT1 phosphorylation by both type I interferon (IFN)-dependent and type I IFN-independent pathways. *J. Virol.* **86,** 12760–12769
43. Qu, J., Hou, Z., Han, Q., Zhang, C., Tian, Z., and Zhang, J. (2013) Poly(I:C) exhibits an anti-cancer effect in human gastric adenocarcinoma cells which is dependent on RLRs. *Int. Immunopharmacol.* **17,** 814–820
44. Inao, T., Harashima, N., Monma, H., Okano, S., Itakura, M., Tanaka, T., Tajima, Y., and Harada, M. (2012) Antitumor effects of cytoplasmic delivery of an innate adjuvant receptor ligand, poly(I:C), on human breast cancer. *Breast Cancer Res. Treat.* **134,** 89–100
45. Besch, R., Poeck, H., Hohenauer, T., Senft, D., Häcker, G., Berking, C., Hornung, V., Endres, S., Ruzicka, T., Rothenfusser, S., and Hartmann, G. (2009) Proapoptotic signaling induced by RIG-I and MDA-5 results in type I interferon-independent apoptosis in human melanoma cells. *J. Clin. Invest.* **119,** 2399–2411
46. Gitlin, L., Barchet, W., Gilfillan, S., Cella, M., Beutler, B., Flavell, R. A., Diamond, M. S., and Colonna, M. (2006) Essential role of mda-5 in type I IFN responses to polyriboinosinic:polyribocytidylic acid and encephalomyocarditis picornavirus. *Proc. Natl. Acad. Sci. U.S.A.* **103,** 8459–8464
47. Myskiw, C., Arsenio, J., Booy, E. P., Hammett, C., Deschambault, Y., Gibson, S. B., and Cao, J. (2011) RNA species generated in vaccinia virus infected cells activate cell type-specific MDA5 or RIG-I dependent interferon gene transcription and PKR dependent apoptosis. *Virology* **413,** 183–193
48. Cirri, P., Chiarugi, P., Marra, F., Raugei, G., Camici, G., Manao, G., and Ramponi, G. (1997) c-Src activates both STAT1 and STAT3 in PDGF-stimulated NIH3T3 cells. *Biochem. Biophys. Res. Commun.* **239,** 493–497
49. Andersen, P., Pedersen, M. W., Woetmann, A., Villingshøj, M., Stockhausen, M. T., Odum, N., and Poulsen, H. S. (2008) EGFR induces expression of IRF-1 via STAT1 and STAT3 activation leading to growth arrest of human cancer cells. *Int. J. Cancer* **122,** 342–349
50. Hsieh, M. Y., Chang, M. Y., Chen, Y. J., Li, Y. K., Chuang, T. H., Yu, G. Y., Cheung, C. H., Chen, H. C., Maa, M. C., and Leu, T. H. (2014) The inducible nitric-oxide synthase (iNOS)/Src axis mediates Toll-like receptor 3 tyrosine 759 phosphorylation and enhances its signal transduction, leading to interferon-β synthesis in macrophages. *J. Biol. Chem.* **28,** 9208–9220
51. Into, T., and Shibata, K. (2005) Apoptosis signal-regulating kinase 1-mediated sustained p38 mitogen-activated protein kinase activation regulates mycoplasmal lipoprotein- and staphylococcal peptidoglycan-triggered Toll-like receptor 2 signalling pathways. *Cell. Microbiol.* **7,** 1305–1317
52. Su, H. L., Liao, C. L., and Lin, Y. L. (2002) Japanese encephalitis virus infection initiates endoplasmic reticulum stress and an unfolded protein response. *J. Virol.* **76,** 4162–4171
53. Peters, K., Chattopadhyay, S., and Sen, G. C. (2008) IRF-3 activation by sendai virus infection is required for cellular apoptosis and avoidance of persistance. *J. Virol.* **82,** 3500–3508

54. Chattopadhyay, S., Marques, J. T., Yamashita, M., Peters, K. L., Smith, K., Desai, A., Williams, B. R., and Sen, G. C. (2010) Viral apoptosis is induced by IRF-3-mediated activation of Bax. *EMBO J.* **29,** 1762–1773
55. Chattopadhyay, S., Fensterl, V., Zhang, Y., Veleeparambil, M., Yamashita, M., and Sen, G. C. (2013) Role of interferon regulatory factor 3-mediated apoptosis in the establishment and maintenance of persistent infection by Sendai virus. *J. Virol.* **87,** 16–24
56. Gambara, G., Desideri, M., Stoppacciaro, A., Padula, F., De Cesaris, P., Starace, D., Tubaro, A., Del Bufalo, D., Filippini, A., Ziparo, E., and Riccioli, A. (2014) TLR3 engagement induces IRF-3-dependent apoptosis in androgen-sensitive prostate cancer cells and inhibits tumor growth *in vivo*. *J. Cell. Mol. Med.* 10.1111/jcmm.12379
57. Vince, J. E., and Tschopp, J. (2010) IRF-3 partners Bax in a viral-induced dance macabre. *EMBO J.* **29,** 1627–1628
58. Yount, J. S., Moran, T. M., and López, C. B. (2007) Cytokine-independent upregulation of MDA5 in viral infection. *J. Virol.* **81,** 7316–7319
59. Zhou, Y., Guo, M., Wang, X., Li, J., Wang, Y., Ye, L., Dai, M., Zhou, L., Persidsky, Y., and Ho, W. (2013) TLR3 activation efficiency by high or low molecular mass poly I:C. *Innate Immun.* **19,** 184–192
60. Hafner, A. M., Corthésy, B., and Merkle, H. P. (2013) Particulate formulations for the delivery of poly(I:C) as vaccine adjuvant. *Adv. Drug Deliv. Rev.* **65,** 1386–1399